PNAS RESEARCH ARTICLE | BIOCHEMISTRY BIOPHYSICS AND COMPUTATIONAL BIOLOGY OPEN ACCESS

Origin recognition complex harbors an intrinsic nucleosome remodeling activity

Sai Li[a], Michael R. Wasserman[a,1], Olga Yurieva[b], Lu Bai[c,d], Michael E. O'Donnell[b,2], and Shixin Liu[a,2]

Contributed by Michael E. O'Donnell; received July 6, 2022; accepted September 13, 2022; reviewed by Sebastian Deindl and Zvi Kelman

Eukaryotic DNA replication is initiated at multiple chromosomal sites known as origins of replication that are specifically recognized by the origin recognition complex (ORC) containing multiple ATPase sites. In budding yeast, ORC binds to specific DNA sequences known as autonomously replicating sequences (ARSs) that are mostly nucleosome depleted. However, nucleosomes may still inhibit the licensing of some origins by occluding ORC binding and subsequent MCM helicase loading. Using purified proteins and single-molecule visualization, we find here that the ORC can eject histones from a nucleosome in an ATP-dependent manner. The ORC selectively evicts H2A-H2B dimers but leaves the $(H3\text{-}H4)_2$ tetramer on DNA. It also discriminates canonical H2A from the H2A.Z variant, evicting the former while retaining the latter. Finally, the bromo-adjacent homology (BAH) domain of the Orc1 subunit is essential for ORC-mediated histone eviction. These findings suggest that the ORC is a bona fide nucleosome remodeler that functions to create a local chromatin environment optimal for origin activity.

origin recognition complex | nucleosome | nucleosome remodeling | DNA replication | origin of replication

DNA replication is a vital life process for all cell types—bacterial, eukaryotic, and archaeal. While there are important differences among the replication proteins of the three domains of life, they mostly function in similar ways. All of them use an origin binding protein that acts with other factors to load two hexameric helicases onto DNA for bidirectional unwinding of the duplex, and thus the ability to simultaneously replicate both strands of the cellular genome (1–3). The eukaryotic origin binding protein is a heterohexamer referred to as the origin recognition complex (ORC) (4). The sequences of the Orc1-6 subunits are conserved from yeast to human, and several of the subunits contain an adenosine triphosphate (ATP)-binding AAA^+ module as in the *Escherichia coli* DnaA initiator. Origins in the budding yeast *Saccharomyces cerevisiae* occur in 100- to 200-bp DNA regions known as autonomously replicating sequences (ARSs) (5–10). However, the existence of ARSs is limited to only some species of budding yeast. Origins of replication with defined DNA sequences are not known at this time to exist in other eukaryotes (1, 2).

The special feature of a defined origin sequence in *S. cerevisiae* has facilitated extensive characterization of the mechanism of DNA replication initiation (1). ORC interacts with Cdc6, Cdt1, and the minichromosome maintenance protein complex (Mcm)2–7 heterohexamer to assemble a Mcm2-7 double hexamer (referred to here as MCM DH) onto DNA in G1 phase (1–3). The loaded MCM DH is the "licensing" factor for replication because it acts as the marker for origin firing in S phase (11). Specifically, the MCM DH is acted upon by several initiation factors to form 2 larger 11-subunit CMG (Cdc45/Mcm2-7/GINS) helicases (12, 13). The two CMG helicases are oriented toward and pass each other to unwind DNA, and recruit the replicative machinery to form bidirectional replication forks (14, 15). ORC and the many other factors required to license an origin and form bidirectional replication forks are conserved in all eukaryotes.

The yeast ARS is AT rich, which is not favorable to nucleosome binding (16, 17). Indeed, chromatin immunoprecipitation sequencing (ChIP-seq) studies indicate that many ARSs have a nucleosome-free region (NFR) that expands in G1/S phase (10, 18–20). Presumably the nucleosomes are moved aside to make way for ORC-mediated MCM DH formation at origins in G1 phase, and for CMG formation in S phase. In vitro studies demonstrate that in the presence of saturating nucleosomes, the ARS is functional for replication initiation without need for classic nucleosome remodelers (21), indicating that the expansion of the NFR at an ARS site may be achieved intrinsically by the origin recognition and replication machinery.

We have recently reported that ORC binding to nucleosomes facilitates the loading of MCM DHs onto DNA, regardless of the DNA sequence (22). In that study, we

Significance

Nucleosomes package the entire eukaryotic genome, yet enzymes need access to the DNA for numerous metabolic activities, such as replication and transcription. Eukaryotic origins of replication in *Saccharomyces cerevisiae* are AT rich and are generally nucleosome free for the binding of ORC (origin recognition complex). However, the nucleosome-free region often undergoes expansion during G1/S phase, presumably to make room for MCM double-hexamer formation that nucleates the 11-subunit helicase, CMG (Cdc45, Mcm2–7, Cdc45). While nucleosome remodelers could perform this function, *in vitro* studies indicate that nucleosome remodeling may be intrinsic to the replication machinery. Indeed, we find here that ORC contains an intrinsic nucleosome remodeling activity that is capable of ATP-stimulated removal of H2A-H2B from nucleosomes.

Reviewers: S.D., Uppsala Universitet; and Z.K., National Institute of Standards and Technology

The authors declare no competing interest.

[1]Present address: Syros Pharmaceuticals, Cambridge, MA 02140.

[2]To whom correspondence may be addressed. Email: odonnel@rockefeller.edu or shixinliu@rockefeller.edu.

This article contains supporting information online at http://www.pnas.org/lookup/suppl/doi:10.1073/pnas.2211568119/-/DCSupplemental.

Published October 10, 2022.

observed the loss of the fluorescently labeled histone signal after ORC–nucleosome interaction, but did not investigate further the source and mechanism of this observation as it was not the focus of the study. Considering that ORC binding is the first step of origin licensing and that ORC harbors multiple ATPase sites, here, we explored the possibility that ORC itself may possess an ATP-facilitated nucleosome remodeling activity. Using single-molecule fluorescence microscopy combined with optical trapping, we find that ORC is indeed an ATP-dependent nucleosome remodeler with the ability to eject H2A-H2B dimers. ORC-mediated nucleosome remodeling may represent the inaugural event toward creating a local chromatin environment permissive to replication initiation.

Results

Experimental Design. This report seeks to examine the fate of core histone subunits within a nucleosome located at either ARS or non-ARS DNA upon *S. cerevisiae* ORC binding. To this end, we engineered the bacteriophage λ genomic DNA to contain an *S. cerevisiae* ARS1 sequence (9) juxtaposed to a "Widom601" nucleosome positioning sequence (23), such that the 601 sequence is immediately adjacent to the B3 element of ARS1 (Fig. 1*A* and *SI Appendix*, Fig. S1). This 601-ARS1 site, located at ∼70% of the λ DNA length from its left end, is the sole position with a strong ACS element, as the λ DNA itself does not contain any strong ACS elements (22). The $\lambda_{601\text{-}ARS1}$ DNA is biotinylated on both ends and tethered between a pair of streptavidin-coated beads held by optical traps (Fig. 1*A*). We assembled reconstituted histone octamers on DNA to form nucleosomes using the histone chaperone Nap1 (24, 25). In this study we used *Xenopus laevis* histone proteins expressed in *E. coli* because their assembly into nucleosomes has been well documented (26). We have previously generated single-cysteine constructs for site-specific fluorophore labeling of either H2A, H2B, or H3 histone subunits (*SI Appendix*, Fig. S2) (22, 27). Histone protein sequences are largely conserved between *S. cerevisiae* and *X. laevis* (*SI Appendix*, Fig. S3), and we have shown in a separate report that *S. cerevisiae* and *X. laevis* nucleosomes are comparable in their ability to direct ORC function in MCM double-hexamer assembly with Cdc6 and Cdt1 (22).

Our in situ nucleosome assembly procedure using fluorescently labeled histone octamers yielded 1 to 7 nucleosome foci per tether (*SI Appendix*, Fig. S4), having nucleosomes at both the 601-ARS1 site and other non-ARS1 DNA sites. Due to the ambiguity in tether orientation, we assumed a nucleosome to be ARS1 adjacent and 601 positioned if it was located at 70% tether length from either end of the tether. Fluorescence intensity analysis of the nucleosome foci indicated that most foci contained a mononucleosome (*SI Appendix*, Fig. S4). Nucleosomes were stably bound to DNA and remained stationary throughout our typical observation time window (∼400 s). Nucleosome assembly was confirmed by the force-extension curves of the tethers, which showed characteristic nucleosome unwrapping transitions at ∼20 pN of pulling force (*SI Appendix*, Fig. S5). The fact that nucleosomes were formed at various locations within the $\lambda_{601\text{-}ARS1}$ DNA template allowed us to compare the consequences of ORC–nucleosome interaction at the ARS1 site versus at non-ARS1 sequences.

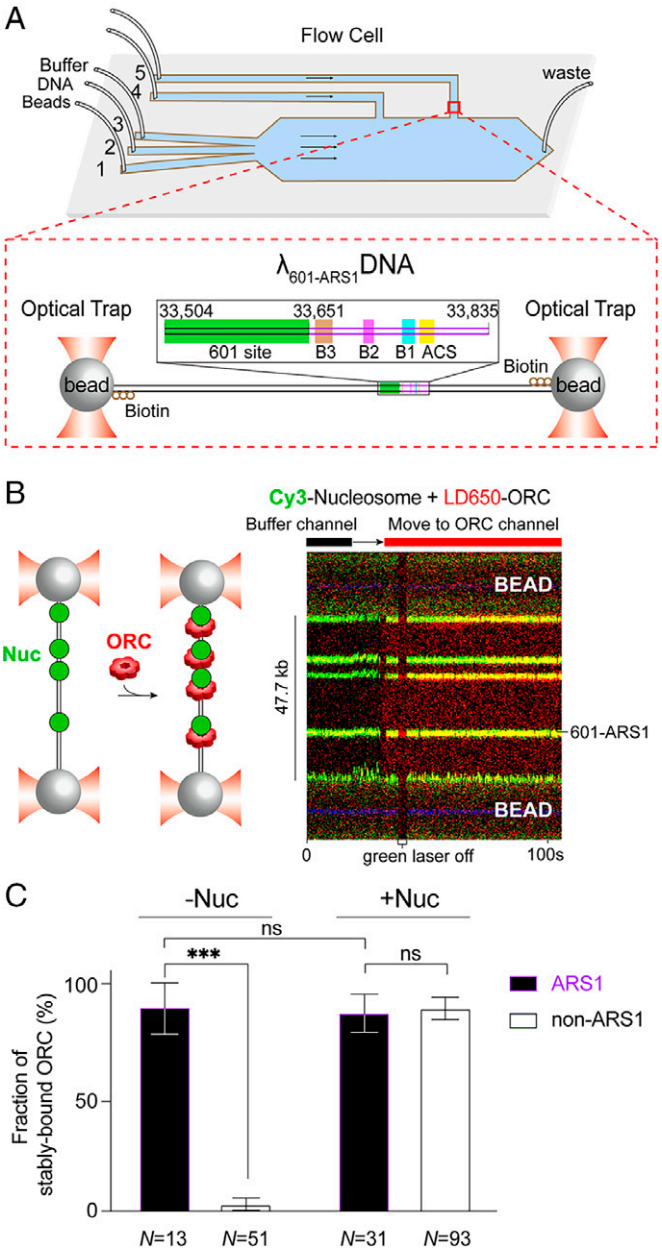

Fig. 1. ORC-Cdc6 stably binds to nucleosomes at the ARS1 site and non-ARS1 sites. (*A*) Schematic of the single-molecule experimental setup and the biotinylated $\lambda_{601\text{-}ARS1}$ DNA template for ORC-nucleosome binding assays. The flow cell contains 3 laminar-flow channels. Two streptavidin-coated beads were optically trapped in channel 1 and then moved into channel 2 that contained biotinylated λ DNA. The tethered λ DNA was then moved to channel 3, containing only buffer to confirm single-tether force-extension characteristics. Cy3-labeled nucleosomes were then assembled onto the DNA in channel 4 and LD650-labeled ORC binding assessed in channel 5. (*B*) Representative kymograph showing Cy3-H2B-nucleosomes (green) on $\lambda_{601\text{-}ARS1}$ DNA between two optically trapped beads (DNA was not directly visualized in this case since there was no DNA-staining dye present). Note that nucleosomes assemble at numerous locations on DNA, not just at the 601 site. Cy3-H2B-nucleosomes (green) and LD650-ORC (red) colocalize, yielding a yellow color. At the indicated region, the green laser is turned off, revealing the presence of the red LD650-ORC signal. (*C*) Quantitation of stably bound ORC-Cdc6 at ARS1 versus non-ARS1 DNA in the absence or presence of nucleosomes. Significance was obtained using an unpaired two-tailed *t* test (ns, not significant; ***$P <$ 0.001). Error bars represent SDs.

ORC Binding to DNA Is Stabilized by Nucleosomes at Any Sequence. To visualize the behavior of ORC on nucleosomal DNA, we inserted a 12-residue "S6" sequence to the N terminus of Orc1, which enables site-specific enzymatic labeling of ORC. The $\lambda_{601\text{-}ARS1}$ DNA template, loaded with Cy3-labeled nucleosomes (shown in green in Fig. 1*B*), was moved to a separate channel containing LD650-labeled ORC (shown in red in Fig. 1*B*). In all of the experiments that used ORC, unlabeled Cdc6 was

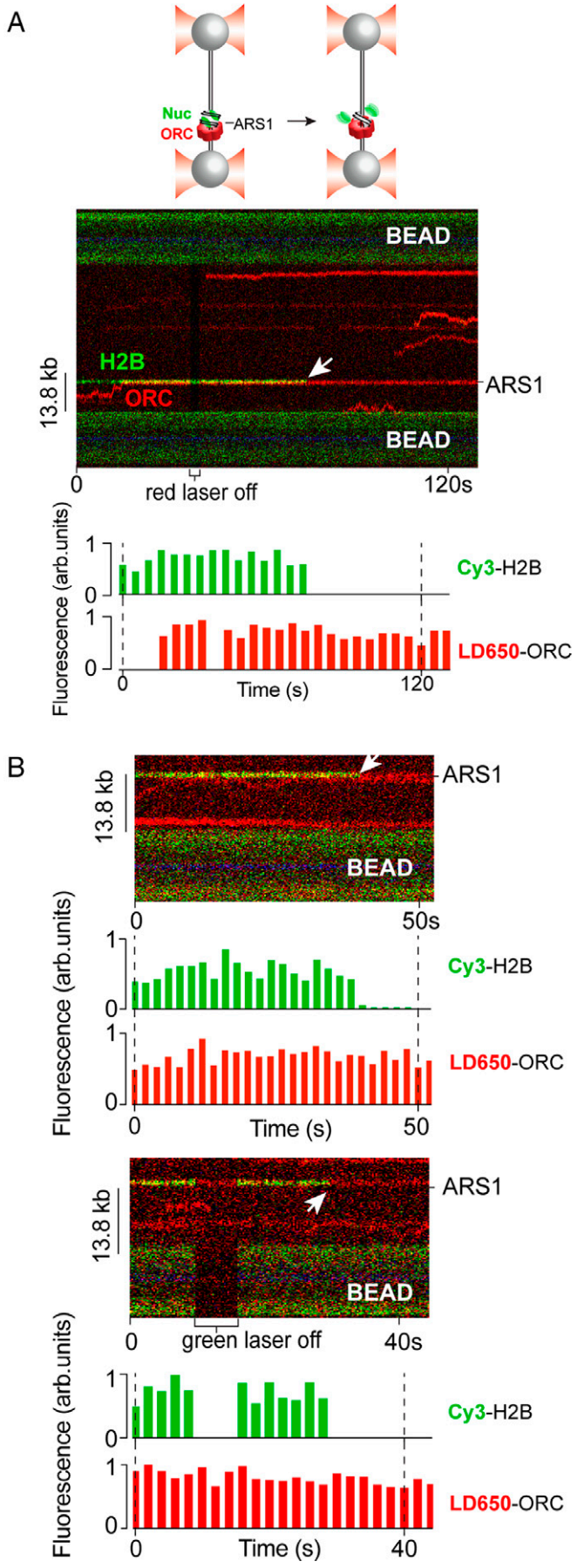

Fig. 2. ORC ejects H2B from nucleosomes assembled adjacent to ARS1. (*A*) Schematic and a representative kymograph showing LD650-ORC (red) in the presence of Cdc6 encountering a Cy3-H2B nucleosome located at the 601-ARS1 site and evicting H2B from the nucleosome (white arrow). The corresponding fluorescence intensities of Cy3-H2B and LD650-ORC at the nucleosome position are plotted below the kymograph. (*B*) Two additional kymographs and the corresponding fluorescence intensity plots showing H2B eviction (loss of the Cy3 signal) from an ARS1-adjacent nucleosome after ORC-nucleosome interaction.

also present, which stabilized ORC binding to DNA (22, 28). We observed that nucleosomes themselves, even those far from ARS1, stabilize the binding of ORC, as shown by the prevalent colocalization of Cy3 and LD650 signals (shown in yellow in Fig. 1*B*). Quantitation of experiments in the presence or absence of nucleosomes showed that ORC-Cdc6 was stabilized at the ARS1 sequence without the presence of nucleosomes, but binding of ORC to non-ARS sites required a nucleosome to form a stable complex (Fig. 1*C*). Below, we examine the nucleosome-ORC complexes formed at the 601-ARS1 site as well as those formed at non-ARS1 sites.

ORC Evicts H2B from Nucleosomes at Both ARS1 and Non-ARS1 Sites. We examined the consequence of ORC–nucleosome interaction at the ARS1 site. In Fig. 2*A*, we show a kymograph in which the DNA tether contained a single nucleosome at the 601-ARS1 position. Upon moving the tether to a channel containing free LD650-ORC in solution, we observed that ORC displayed diffusive motions among non-ARS and non-nucleosome sites, but that one ORC molecule moved to and remained at the 601-ARS1 site, where a nucleosome also resided. The stable association of the "red" ORC binding to a "green" nucleosome at the ARS1 site yields a stationary yellow signal. Unexpectedly, we observed that the yellow color at the 601-ARS1 site, after ~1 min, converted to red, indicating the disappearance of the green fluorescence signal from the histone H2B subunit (Fig. 2*A*). Similar results (i.e., the disappearance of the H2B signal from the ARS1 nucleosome site) were observed on other tethers as well (Fig. 2*B*). We can rule out that this is due to photobleaching of the Cy3 fluorophore on H2B because the H2B fluorescence signal was long-lasting in the absence of ORC, seldomly photobleached by itself within the observation window. It is also unlikely that the loss of the Cy3 signal was caused by fluorescence resonance energy transfer between Cy3-H2B and LD650-ORC, as we did not observe a corresponding increase in the LD650-ORC intensity. Therefore, the most plausible explanation is that H2B is evicted by ORC. Overall, we observed H2B eviction on 47% of the tethers that contained a nucleosome at the ARS1 site.

As demonstrated in Fig. 1, ORC stably associated with all of the nucleosomes regardless of whether the nucleosome was located at ARS1 or was distant from ARS1. With the observation that ORC evicts H2B at the ARS1 site, we examined the cases in which ORC targeted nucleosomes at positions distinct from the ARS1 site. We found that ORC also evicts H2B from nucleosomes at non-ARS1 sites (Fig. 3 *A* and *B*) and, more importantly, the eviction efficiency was similar between ARS1 and non-ARS1 sites (Fig. 3*C*). In these experiments we held the tethers at a low force of 2.5 pN. To further rule out the potential contribution of tension on the DNA tether to histone eviction, we lowered the force to 1 pN and obtained a similar ORC-induced H2B eviction efficiency (*SI Appendix*, Fig. S6).

ORC Also Evicts H2A but Not H3. Given that the H2A-H2B dimer is often processed together as a unit by chromatin remodelers (29), we next examined the fate of histone H2A upon ORC-nucleosome engagement by placing the Cy3 fluorophore

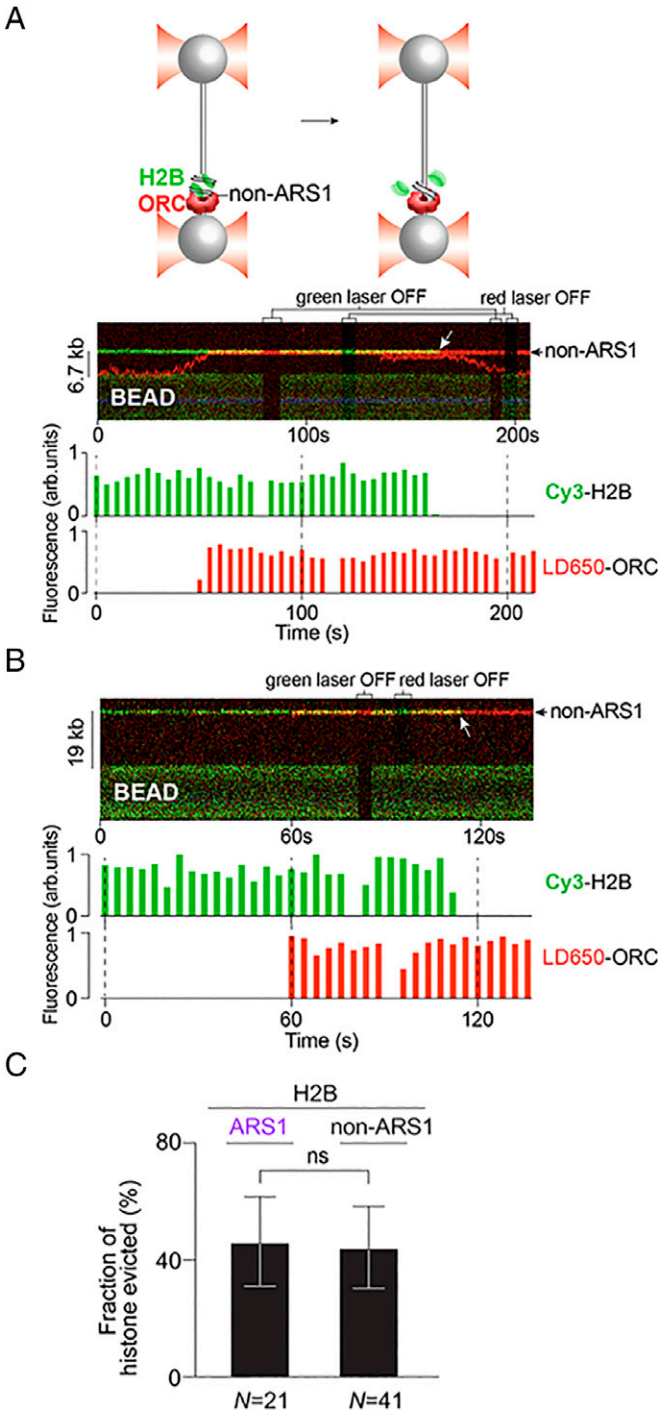

Fig. 3. ORC ejects H2B from nucleosomes at non-ARS sites. (*A* and *B*) Two representative kymographs showing LD650-ORC encountering a Cy3-H2B nucleosome located at a non-ARS1 site via one-dimensional search (*A*) or three-dimensional search (*B*). White arrows indicate the H2B eviction events. The corresponding fluorescence intensity plots are shown below each kymograph. (*C*) Fraction of H2B evicted by ORC at ARS1 versus non-ARS1 sites. Significance was obtained using an unpaired two-tailed *t* test (ns, not significant). Error bars represent SDs.

on H2A. We found that in the absence of ORC, the H2A fluorescence signal persisted at the nucleosome loci throughout the observation window; however, when ORC was present, H2A eviction was frequently observed (Fig. 4 *A* and *B*). Overall, H2A and H2B were ejected at a similar rate: ~40–50% of the dimers were removed by ORC within 400 s (Fig. 4 *B* and *C*).

Next, we asked whether ORC can also destabilize the $(H3\text{-}H4)_2$ tetramer, which in general is much less dynamic within the nucleosome than the H2A-H2B dimers (30). We loaded the $\lambda_{601\text{-}ARS1}$ DNA with nucleosomes containing fluorescently labeled histone H3 and found that, contrary to H2A and H2B, virtually all of the H3 molecules remained on DNA upon ORC binding at both ARS1 and non-ARS1 sites (Fig. 4*D*). This result is corroborated by the normalized fluorescence intensities averaged over many nucleosomal loci, showing an ORC-dependent decrease over time for H2A and H2B, but not for H3 (Fig. 4 *C* and *E*). Therefore, we propose that ORC remodels nucleosomes by selectively removing H2A-H2B dimers rather than disassembling the entire nucleosome. Notably, this proposal can explain the observation that the majority of ORC stayed at the same position after H2A-H2B eviction (Fig. 4*F*)—even at non-ARS1 positions where ORC does not stably bind without nucleosomes (Fig. 3 *A* and *B* and 4*A*)—presumably because the remaining $(H3\text{-}H4)_2$ tetramer can still stably hold ORC.

ORC-Mediated Nucleosome Remodeling Is ATP Dependent. The histone eviction process likely consumes free energy. Therefore, we assessed the role of ATP in the nucleosome remodeling activity of ORC. In accordance with previous results (4, 31), we found that omitting ATP abolished ORC loading on DNA altogether in our single-molecule assay. As described above, in the presence of ATP, we observed significant H2A-H2B eviction from nucleosomes by ORC but negligible H3 eviction (Fig. 5). Using a nonhydrolyzable ATP analog, adenylyl-imidodiphosphate (AMP-PNP), we still observed ORC binding to nucleosomes on tethered DNA but a drastically diminished H2A ejection efficiency (Fig. 5), indicating that ATP hydrolysis is involved in histone eviction by ORC. Thus, the ATPase activity is not only used by ORC for MCM DH loading and pre-RC formation as previously known (1) but it is also required for histone eviction upon ORC–nucleosome interaction, revealing that ORC is a bona fide, albeit limited, chromatin remodeler.

ORC Alters Nucleosomal DNA Accessibility. Our single-molecule results predict that ORC binding renders part of the nucleosomal DNA more accessible due to H2A-H2B dissociation. To test this prediction, we performed a restriction enzyme accessibility assay with a reconstituted mononucleosome positioned next to an ARS1 DNA sequence (*SI Appendix*, Fig. S7*A*). We evaluated the cleavage efficiency of BanI, whose restriction site is located within the nucleosome 18 bp from the ARS1-proximal nucleosomal DNA end. We found that the addition of ORC and ATP led to significantly enhanced BanI cleavage compared to the control condition where ATP was omitted (*SI Appendix*, Fig. S7*B*), suggesting that the BanI site becomes more exposed upon nucleosome remodeling by ORC. We then performed the same assay with a different enzyme, BsiWI, whose restriction site is located close to the nucleosome dyad. In this case, we did not detect a significant enhancement of BsiWI cleavage induced by ORC and ATP (*SI Appendix*, Fig. S7*C*). These results are consistent with our model that ORC selectively removes H2A-H2B dimers, making the outer turn of nucleosomal DNA more accessible while leaving the $(H3\text{-}H4)_2$-bound inner turn occluded. In this regard, ORC is distinctive from other remodelers such as ISW1a, which slides the entire histone octamer relative to the DNA (32). Indeed, ISW1a enhanced both BanI and BsiWI cleavage in our experiments (*SI Appendix*, Fig. S7 *B* and *C*).

ORC Does Not Remodel H2A.Z-Containing Nucleosomes. H2A.Z is a major histone H2A variant enriched at the boundaries of NFRs—including replication origins—and plays an

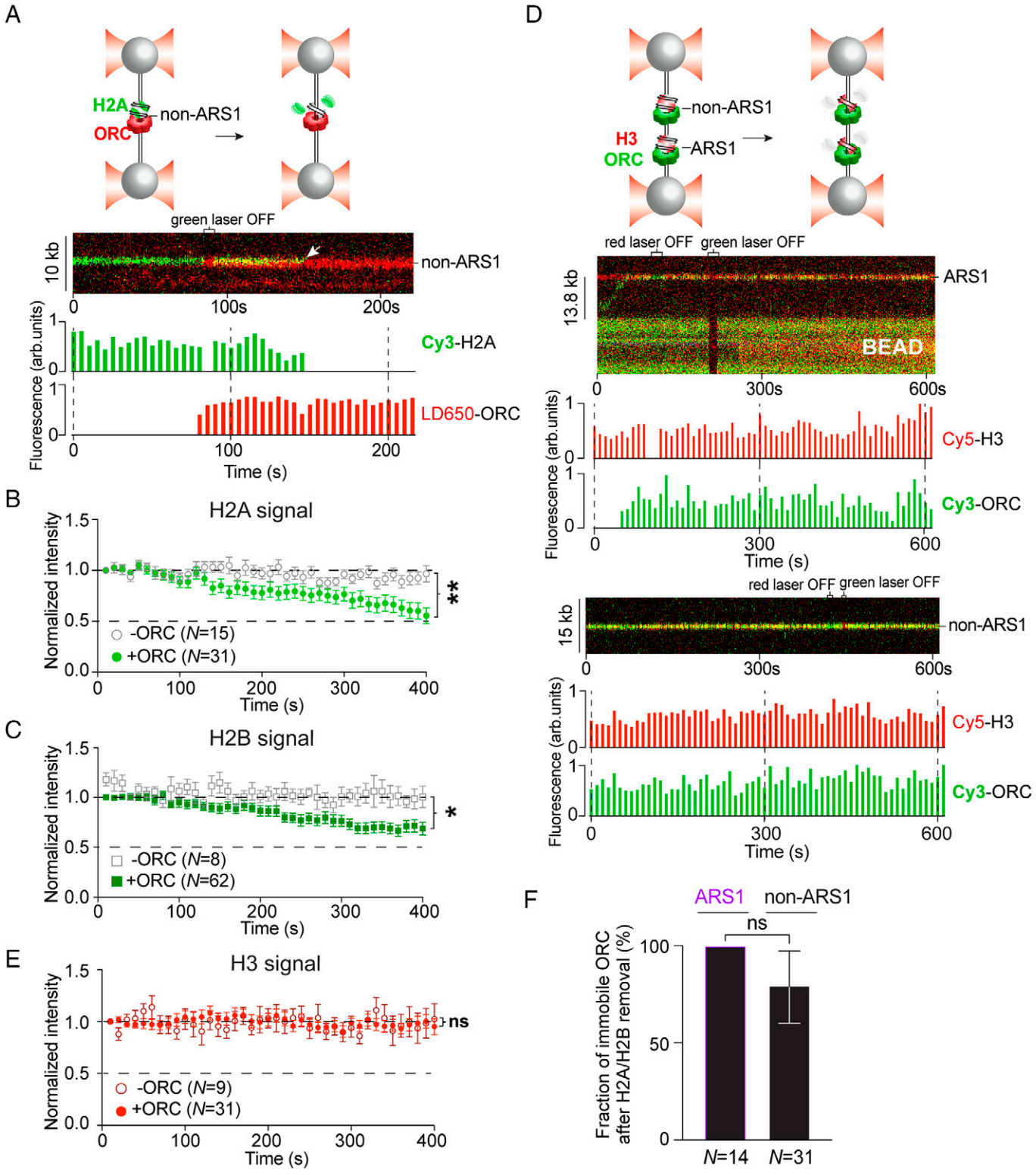

Fig. 4. ORC also ejects H2A but not H3. (*A*) A representative kymograph showing LD650-ORC encountering a nucleosome at a non-ARS1 site and evicting Cy3-H2A from it. The corresponding fluorescence intensity plots are shown below. (*B* and *C*) Normalized average intensity of H2A (*B*) and H2B (*C*) fluorescence signal at nucleosome sites as a function of time in the absence or presence of ORC. *N* indicates the number of nucleosomes analyzed for each condition. (*D*) Two representative kymographs of Cy3-ORC encountering a Cy5-H3 nucleosome at an ARS1 (*Top*) or non-ARS1 (*Bottom*) site. The corresponding fluorescence intensity plots are shown below each kymograph. (*E*) Normalized average intensity of H3 fluorescence signal at nucleosome sites as a function of time in the absence or presence of ORC. Error bars in (*B*), (*C*), and (*E*) represent SEMs. Significance was obtained using an unpaired two-tailed *t* test at the 400-s time point (ns, not significant; $*P < 0.05$; $**P < 0.01$). (*F*) Fraction of nucleosome-bound ORC that remained immobile after H2A/H2B eviction at ARS1 versus non-ARS1 sites. Error bars in (*F*) represent SDs. *N* indicates the number of analyzed events. Significance was obtained using an unpaired two-tailed *t* test (ns, not significant).

important role in the activation of replication origins (19, 33, 34). To investigate the interaction between ORC and H2A.Z nucleosomes, we reconstituted octamers containing Cy3-labeled H2A.Z and formed H2A.Z nucleosomes on $\lambda_{601\text{-}ARS1}$ DNA. Upon adding LD650-labeled ORC, we observed that ORC still associated stably with H2A.Z nucleosomes (Fig. 6 *A* and *B*).

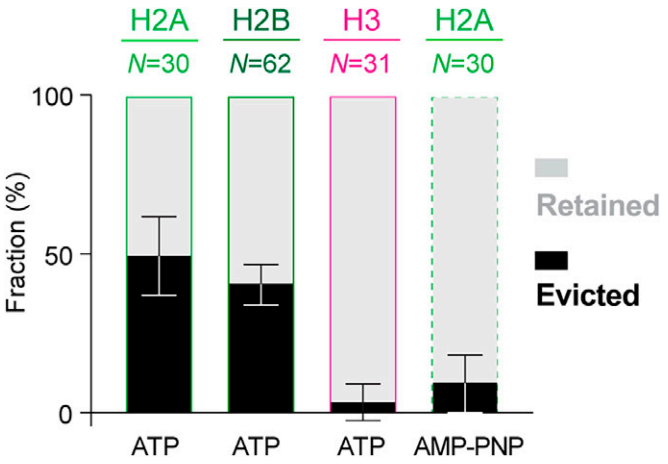

Fig. 5. Requirement of ATP hydrolysis for the nucleosome remodeling activity of ORC. Fraction of histones (H2A, H2B, or H3) evicted versus retained upon ORC–nucleosome interaction in the presence of ATP or AMP-PNP. Error bars represent SDs.

However, this stable interaction did not displace any H2A.Z molecules during the entire observation period (Fig. 6*C*), in striking contrast to the efficient ejection of canonical H2A by ORC.

Nucleosome Remodeling Activity of ORC Depends on the Orc1 BAH Domain. A known contact between ORC and the nucleosome is the bromo-adjacent homology (BAH) domain of Orc1, which is conserved across eukaryotes and is a common motif in chromatin remodelers (29). Structural analyses revealed that the BAH domain contacts all four core histones (35, 36). The Orc1 BAH domain is not essential to viability, but the deletion of Orc1 BAH in the cell results in a genome-wide change in origin usage (37). To investigate the role of BAH in ORC-mediated nucleosome remodeling, we used CRISPR-Cas9 to generate a BAH-deleted *S. cerevisiae* strain, and purified and labeled the ORC$^{\Delta BAH}$ complex for single-molecule experiments (Fig. 7*A* and *SI Appendix*, Fig. S2). We observed that ORC$^{\Delta BAH}$ still stably binds nucleosomes (Fig. 7 *B* and *C*), consistent with previous results (38), presumably through other ORC–nucleosome connections. However, ORC$^{\Delta BAH}$ displayed a significantly impaired H2A-H2B eviction efficiency (Fig. 7 *B* and *D*), suggesting that BAH is critical for the nucleosome remodeling activity of ORC. These results indicate that nucleosome association and remodeling are two separate activities of ORC, each presumably mediated by a distinct set of motifs or subunits in the ORC complex.

ORC Affects Genome-Wide Nucleosome Composition. Finally, to investigate whether ORC-mediated nucleosome remodeling observed in vitro also occurs in the cell, we analyzed in vivo nucleosome composition over genome-wide ORC binding sites based on published datasets. We identified 1,000 top-ranked ORC binding sites based on the *S. cerevisiae* Orc1 ChIP-seq data (19, 39, 40) and sorted them into two groups based on their peak intensities. Next, we analyzed the *S. cerevisiae* MNase-histone ChIP-seq data (41). In this dataset, the MNase-seq signal ("input") reflects the degree of protection against micrococcal nuclease digestion at a given genomic site; the subsequent histone ChIP-seq signal ("IP") reflects the level of a certain histone in the protected nucleosomal particles at the corresponding site. Nucleosome composition can thus be evaluated by calculating the ratio between IP and input (Fig. 8*A*). Over the highly ranked Orc1 sites, the average H4 content is centered around 1, the normalized genome-average level generated from the IP/input values for 10,000 randomly selected sites. Significantly, the average H2B content at strong Orc1 sites is depleted to 0.6–0.7 (Fig. 8 *B*–*D*). In contrast, over the lower ranked Orc1 sites (weak ORC binding or false positive sites), the H2B and H4 contents have very similar distributions. This analysis supports the model that strong ORC binding induces selective H2A-H2B depletion in nearby nucleosomes.

Discussion

ORC Is a Nucleosome Remodeler. In this report, we identify an ATP-dependent activity of ORC that may apply to all eukaryotes. We demonstrate that ORC binding to the nucleosome or the linker DNA destabilizes histone wrapping and can evict H2A-H2B dimers from the nucleosome, thus adding ORC to the known list of chromatin remodelers. This diverse family of enzymes alters chromatin by repositioning nucleosomes, ejecting part of or full octamers, or editing histone subunits (29). We show that ORC is able to evict H2A-H2B dimers—but not the entire octamer—from the nucleosome. Notably, most of the H2A/H2B eviction events occurred in a single step, as shown in

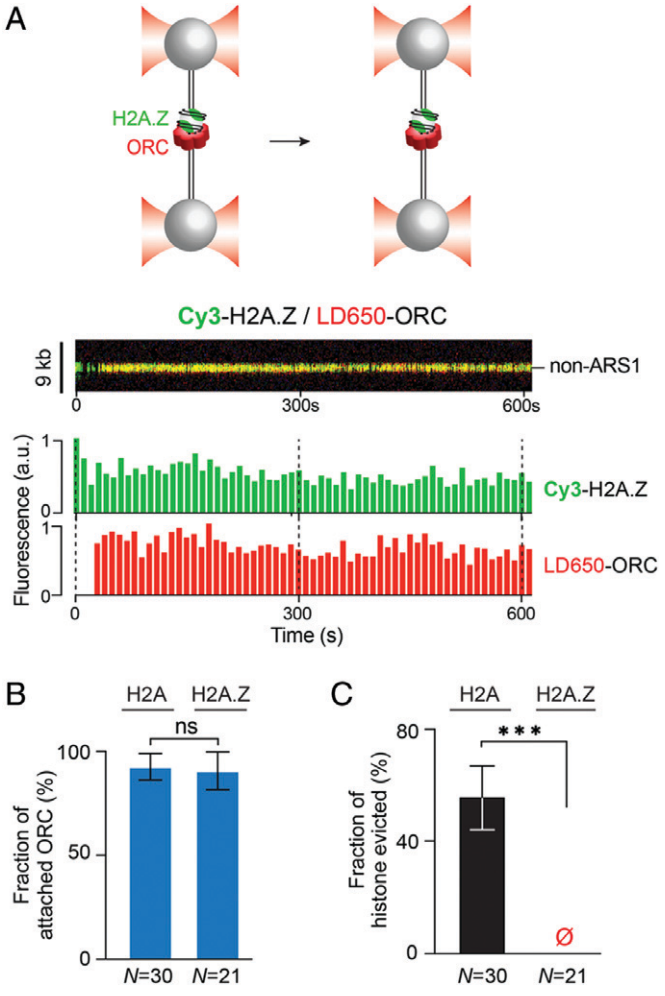

Fig. 6. ORC differentially remodels H2A and H2A.Z nucleosomes. (*A*) Schematic and a representative kymograph of LD650-ORC (red) encountering a Cy3-H2A.Z nucleosome (green). The corresponding fluorescence intensity plots are shown below the kymograph. (*B*) Fraction of ORC that remained stably bound to H2A versus H2A.Z nucleosomes. (*C*) Fraction of H2A versus H2A.Z evicted upon ORC–nucleosome interaction. *N* indicates the number of analyzed events. Significance was obtained using an unpaired two-tailed *t* test (ns, not significant; ***$P < 0.001$). Error bars represent SDs.

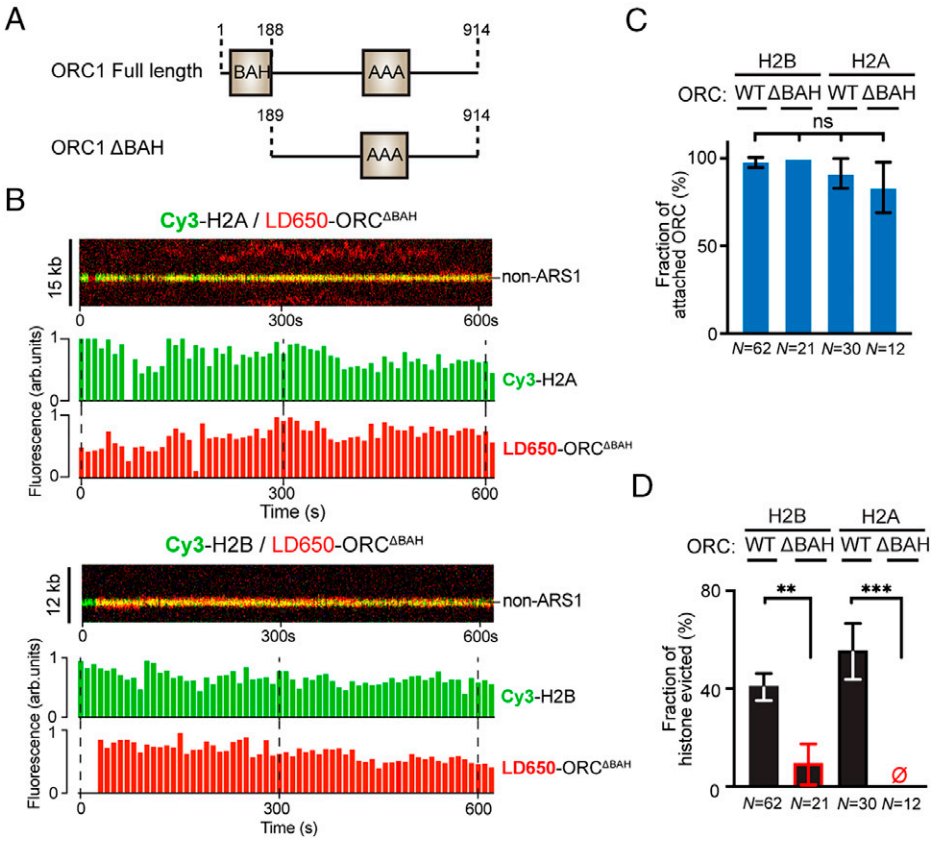

Fig. 7. The nucleosome remodeling activity of ORC depends on the BAH domain of Orc1. (*A*) Schematic of the full-length Orc1 and Orc1$^{\Delta BAH}$. (*B*) Two representative kymographs of LD650-ORC$^{\Delta BAH}$ (red) encountering a Cy3-H2A or Cy3-H2B nucleosome (green). The corresponding fluorescence intensity plots are shown below each kymograph. (*C*) Fraction of ORC or ORC$^{\Delta BAH}$ that stably bound to Cy3-H2B or Cy3-H2A nucleosomes for at least 400 s. (*D*) Fraction of H2B or H2A evicted upon ORC or ORC$^{\Delta BAH}$ interaction with a nucleosome. *N* indicates the number of analyzed events. Significance was obtained using an unpaired two-tailed *t* test (ns, not significant; $^{**}P < 0.01$; $^{***}P < 0.001$). Error bars represent SDs.

the example kymographs in Figs. 2–4. This observation indicates that both H2A-H2B dimers are evicted simultaneously or one following the other in quick succession beyond our time resolution (500 ms), which would distinguish ORC from remodelers that exchange the two dimers independently. However, some of the single-step eviction events could also be explained by imperfect labeling or the presence of hexasomes in our sample.

We also show that ORC discriminates between H2A and H2A.Z, ejecting the former but retaining the latter. It will be interesting to examine whether ORC has a nucleosome editing activity by replacing canonical H2A-H2B dimers with H2A.Z-H2B dimers, akin to the yeast SWR1 (42). It also remains to be determined whether ORC can slide nucleosomes, as the current resolution of our assay prohibited us from discerning small movements on DNA that are within the diffraction limit.

We presume that the remodeling activity of ORC is specifically targeted to replication initiation sites, thus limiting its use compared to more global nucleosome remodeling over large areas of the genome performed by other nucleosome remodelers. ORC ejects approximately 40–50% of H2A-H2B from nucleosomes under our experimental conditions. It is not clear whether ORC must remove histone subunits for in vivo function, or whether instead it may loosen histone-DNA contacts to move the nucleosome a short distance on the 100- to 200-bp ARS region for MCM DH assembly. In support of the ejection/moving hypothesis, our genomic analysis reveals that nucleosomes at many origins appear to lack H2A-H2B. While speculative, it is possible that ORC destabilizes H2A-H2B and thereby facilitates the incorporation of the H2A.Z variant, which we show here is more stable upon ORC binding than canonical H2A and is known to be enriched in nucleosomes flanking ARS regions (33).

The ATPase Sites in ORC. Five of the six ORC subunits contain an AAA$^+$ ATPase site (43). Hydrolysis in only one ATPase site (i.e., Orc1) is required for the formation of the MCM DH on nucleosome-free DNA (1, 2). Thus, there is potential for further ATPase site usage for ORC function, such as on chromatinized DNA. Considering their structural divergence, ORC may function differently from other chromatin remodelers. For example, ORC-mediated nucleosome remodeling may only affect adjacent nucleosomes, while the switch/sucrose non-fermentable (SWI/SNF) family of remodelers acts over large regions of the genome for transcriptional regulation and chromosome organization (29). At present, the ATPase site of the Orc1 subunit is implicated in pre-RC formation on DNA lacking nucleosomes, but the individual ATPase site functions of the other ORC subunits remain uncertain (1). We currently do not know which subunit(s) of ORC are responsible for the ATP-stimulated H2A-H2B eviction. This will be an important subject for future investigation.

Orc1 BAH Domain. The BAH domain of Orc1 is an established connection of ORC to all four core histones in the nucleosome (35, 36). It is noteworthy, however, that even upon removal of the BAH domain, the ORC$^{\Delta BAH}$ mutant still binds to nucleosomes (38), and this is recapitulated in our single-molecule assay. These results imply that ORC engages with nucleosomes through other points of contact in addition to the BAH domain.

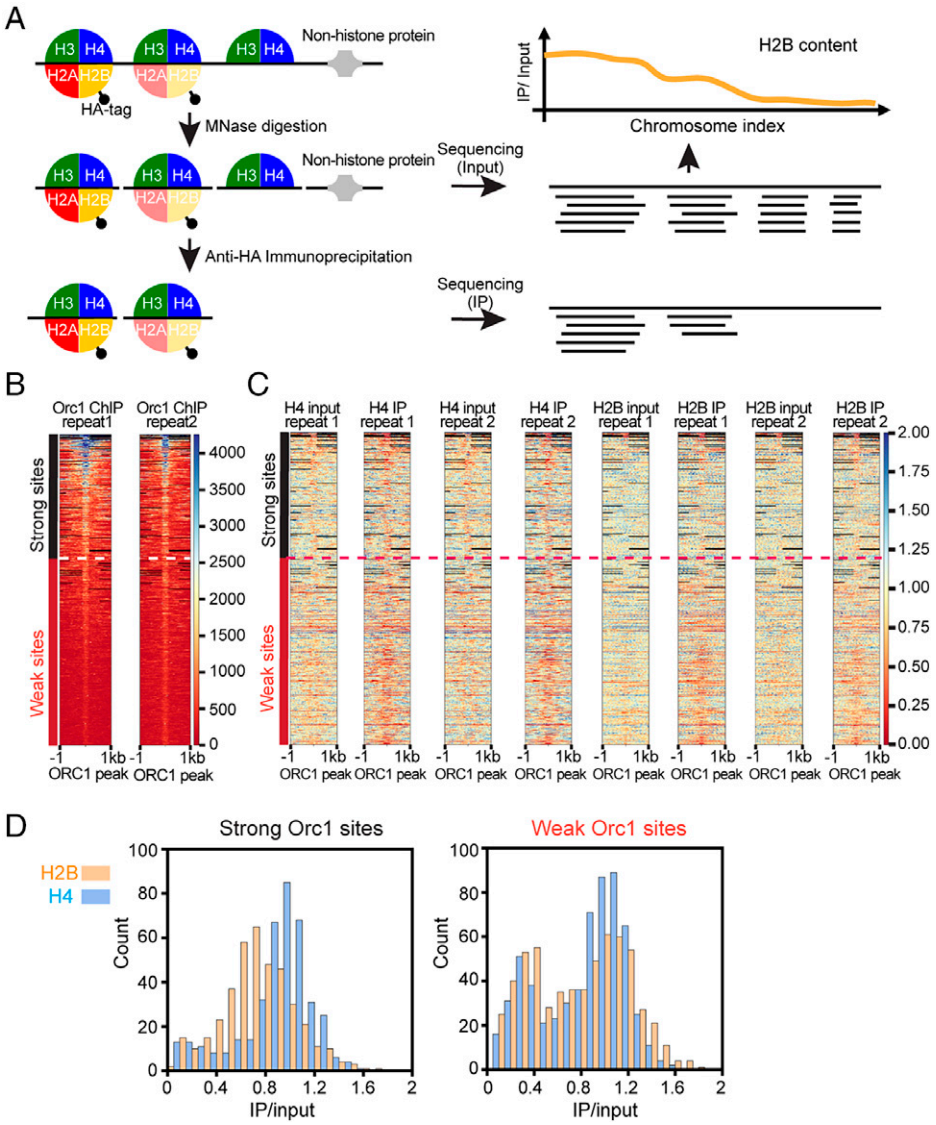

Fig. 8. H2B is depleted at strong ORC binding sites genome-wide. (*A*) Workflow of analyzing specific histone content in the *S. cerevisiae* genome. The diagram shows the situation in which H2B is hemagglutinin (HA) tagged. The same procedure applies to HA-tagged H4. (*B*) Heatmap of the Orc1 ChIP-seq data (19) aligned at the center of Orc1 peaks and sorted based on the peak intensity (ranked 1 to 1,000 from *Top* to *Bottom*). The two panels represent biological replicates. (*C*) Heatmap of the H4/H2B MNase-ChIP-seq data (41) at the top 1,000 Orc1 sites. The heatmaps are aligned at the center of Orc1 peaks with the same rank order as in (*B*). Different panels represent replicates of MNase-seq (input) and MNase-H4/H2B ChIP-seq (IP) datasets. (*D*) Histograms of the normalized H2B and H4 content (estimated by IP/input) over strong (*Left*; ranked 1 to 400) and weak (*Right*; ranked 401 to 1,000) Orc1 binding sites.

Identification of these additional contacts between ORC and nucleosomes is of obvious biological importance.

An earlier study examined the genome-wide origin usage for $ORC^{\Delta BAH}$ compared to wild-type ORC (37), and found that while the $ORC^{\Delta BAH}$ mutant cells still appeared to grow normally, deletion of the BAH domain had diverse effects on specific origin usage: Many origins became inactive or highly defective, some origins were unaffected, and numerous origins functioned within a continuum between inactive and active states. Thus, the BAH domain is important for normal origin function, consistent with the fact that it is conserved across all eukaryotic species. The impaired H2A-H2B eviction activity of $ORC^{\Delta BAH}$ that we observed here may underlie the altered origin pattern in BAH-deleted *S. cerevisiae* cells. Nonetheless, many ARS origins can be deleted from yeast chromosomes without seriously affecting cell viability or growth (1). Thus, even with the profound impact of BAH deletion on global origin usage, one may expect that those origins that remain active upon BAH deletion will provide sufficient functionality for the cell, at least under laboratory conditions.

Implications of the Chromatin Remodeling Activity of ORC. In light of our finding that nucleosomes provide the primary positional cue for ORC binding (22), the main additional requirement for origin licensing then becomes the existence of an NFR next to the ORC-bound nucleosome for helicase loading. It is known that ORC binding to DNA and the subsequent MCM DH loading in G1 phase correlate with widening of the NFR at an ARS element (18, 20). Biochemical studies have shown that a nucleosome positioned over an ARS element will prevent replication initiation at that ARS origin, and that ARS elements are generally AT rich, which is known to hinder nucleosome occupancy (1, 19, 44). However, while ARSs typically contain a minimal nucleosome-free core region, this NFR is limited and appears to require expansion for full origin function (18, 19). Hence, one may expect that the nucleosome

remodeling activity observed here for ORC is required for or facilitates MCM DH formation. Given that ORC is the first replication factor to bind origins, its inherent nucleosome-remodeling activity may serve as the inaugural event leading to the widening of NFRs at origins and MCM DH formation. Classic SWI/SNF chromatin remodelers have been implicated in replication initiation (45). A recent study showed that MCM DHs can be successfully assembled without SWI/SNF or RSC remodelers, but maturation of the MCM DH to CMG in S phase requires these additional remodelers (24), possibly reflecting the larger size of the CMG helicases that include the MCMs, along with the GINS and Cdc45 proteins. It thus remains possible that ORC may contribute to chromatin remodeling during S phase. Our findings also raise the question of whether nucleosome remodeling mediated by ORC can result in nucleosome editing in which other histone variants replace canonical H2A-H2B, in addition to expanding an NFR. Indeed, consistent with our single-molecule results, H2A.Z nucleosomes are enriched at in vivo origin sites where ORC binds (46).

The activity of ORC to evict H2A-H2B dimers may also be involved in transcriptional regulation. Specifically, the Orc1 BAH domain is known to be required for epigenetic silencing at budding yeast heterochromatin domains such as the mating-type loci (47). ORC-mediated nucleosome remodeling may initiate events, possibly in coordination with other chromatin factors, to create a local landscape conducive to transcriptional silencing. These chromatin-related events enabled by ORC-nucleosome interplay in yeast and higher organisms are of primary importance to define in future studies.

Materials and Methods

Proteins. Yeast Cdc6, ORC, S6-ORC, and Nap1 were expressed by recombinant means and purified as previously described (22). Sfp synthase was purified as previously described (48). The S6-ORC$^{\Delta BAH}$ expression strain was made using CRISPR-Cas editing of the S6-ORC strain (22), as detailed in the *SI Appendix*, and purification of S6-ORC$^{\Delta BAH}$ was similar to S6-ORC, as detailed in the *SI Appendix*. Recombinant *X. laevis* histones and histone mutants (single-cysteine constructs H2A K120C, H2B T49C, H3 G33C+C110A, and H2A.Z K15C) were made and purified as previously described (27); further details may be found in the *SI Appendix*.

Fluorescent Labeling of Proteins. S6-ORC and S6-ORC$^{\Delta BAH}$ were labeled using Sfp synthase and Cy3/LD650-CoA (Lumidyne Technologies), as detailed in the *SI Appendix*. Histones were chemically labeled on the single Cys residue using either a Cy3 or Cy5 maleimide (Cytiva), as detailed in the *SI Appendix*.

Single-Molecule Experiments. Single-molecule experiments were performed on a LUMICKS C-Trap instrument (48). Preparation of $\lambda_{601\text{-}ARS1}$ DNA and assembly of nucleosomes are detailed in the *SI Appendix,* which also includes other details about the experimental procedure.

Genomic Data Analysis. To identify the genome-wide ORC binding sites, we downloaded Orc1 ChIP-seq data from Eaton et al. (19) (SRR034475 and SRR034476), aligned it to the yeast genome (version Scer3) with bowtie2, and used MACS2 to identify the peaks (threshold: effective $P = 0.01$). A total of 1,920 peaks was identified. All of the peaks were resized to 200 bp (±100 bp from the center point) and ranked based on the area underneath the curve. We assigned the top-ranked 400 peaks as "strong" Orc1 binding sites (the original Eaton et al. paper (19) used more stringent criteria and identified 267 peaks). The intermediate group (401–1,000) represents "weak" Orc1 binding sites and was used as a control. The bottom-ranked (1,001–1,920) peaks were discarded.

To investigate the nucleosome composition near Orc1 sites, we analyzed the MNase-histone ChIP-seq data in Chereji et al. (41). In this dataset, the MNase-seq data ("input") reflect the degree of protection against micrococcal nuclease digestion; the MNase-H2B/H4 ChIP-seq data ("IP"), divided by the input, reflect the level of H2B or H4 in the protected particles. We used the "multicovbed" program to calculate the input and IP signals over the sorted Orc1 sites. We also generated 10,000 random regions in the genome, 200 bp in size, performed the same IP/input calculation, and used this value to normalize the histone data. The original data were obtained with different strengths of MNase digestion (e.g., 50 U, 200 U). The IP/input values over Orc1 sites are similar with 50 U or 200 U MNase treatment. The H2B results in this paper were averaged between one 50 U and one 200 U dataset (we had one set of each), and the H4 results were averaged between two 200 U datasets.

Statistical Analysis. Errors reported in this study represent the SD, except that the errors for normalized average intensity represent the SEM. P values were determined from unpaired two-tailed t tests (ns, not significant; $*P < 0.05$; $**P < 0.01$; $***P < 0.001$; $****P < 0.0001$).

Data, Materials, and Software Availability. All of the data are available from the corresponding authors upon request.

All of the data are included in the article and/or supporting information.

ACKNOWLEDGMENTS. We thank L. Langston, R. Mayle, G. Schauer, N. Yao, and D. Zhang in the O'Donnell laboratory and R. Shih in the Liu laboratory for help with reagents; J. Watters in the Liu laboratory for data analysis codes; and other members of the Liu and O'Donnell laboratories for discussions. L.B. is supported by NIH R01GM118682 and R35GM139654. M.E.O. is supported by NIH R01GM115809 and the Howard Hughes Medical Institute. S. Liu is supported by the Robertson Foundation, the Alfred P. Sloan Foundation, the Pershing Square Sohn Cancer Research Alliance, and NIH Director's New Innovator Award DP2HG010510.

Author affiliations: [a]Laboratory of Nanoscale Biophysics and Biochemistry, The Rockefeller University, New York, NY 10065; [b]Laboratory of DNA Replication, The Rockefeller University and Howard Hughes Medical Institute, New York, NY 10065; [c]Department of Biochemistry & Molecular Biology, Center for Eukaryotic Gene Regulation, The Pennsylvania State University, University Park, PA 16802; and [d]Department of Physics, The Pennsylvania State University, University Park, PA 16802

Author contributions: S. Liu and M.E.O. oversaw the project. S. Liu, M.R.W., M.E.O., and S. Li designed research. S. Li, M.R.W., and O.Y. performed research. M.R.W. prepared the DNA templates. M.R.W., O.Y., and S. Li prepared and labeled the replication proteins. S. Li prepared and labeled the nucleosome samples. S. Li and M.R.W. performed single-molecule experiments and analyzed the data. S. Li performed the restriction enzyme accessibility assay. S. Li, M.R.W., and O.Y. contributed reagents/analytic tools. L.B. performed the genomic data analysis. S. Liu, M.R.W., L.B., M.E.O., and S. Li analyzed data. S. Liu, O.Y., L.B., M.E.O., and S. Li wrote the paper.

1. S. P. Bell, K. Labib, Chromosome duplication in *Saccharomyces cerevisiae*. *Genetics* **203**, 1027–1067 (2016).
2. F. Bleichert, M. R. Botchan, J. M. Berger, Mechanisms for initiating cellular DNA replication. *Science* **355**, eaah6317 (2017).
3. M. O'Donnell, L. Langston, B. Stillman, "Principles and concepts of DNA replication in bacteria, archaea, and eukarya" in *DNA Replication*, S. D. Bell, M. Mechali, M. L. DePhamphilis, Eds. (Cold Spring Harbor Laboratory Press, 2013), chap. 1, pp. 1–13.
4. S. P. Bell, B. Stillman, ATP-dependent recognition of eukaryotic origins of DNA replication by a multiprotein complex. *Nature* **357**, 128–134 (1992).
5. D. M. MacAlpine, H. K. Rodríguez, S. P. Bell, Coordination of replication and transcription along a *Drosophila* chromosome. *Genes Dev.* **18**, 3094–3105 (2004).
6. M. K. Raghuraman *et al.*, Replication dynamics of the yeast genome. *Science* **294**, 115–121 (2001).
7. K. Shirahige, T. Iwasaki, M. B. Rashid, N. Ogasawara, H. Yoshikawa, Location and characterization of autonomously replicating sequences from chromosome VI of *Saccharomyces cerevisiae*. *Mol. Cell. Biol.* **13**, 5043–5056 (1993).
8. J. F. Theis, C. S. Newlon, The ARS309 chromosomal replicator of *Saccharomyces cerevisiae* depends on an exceptional ARS consensus sequence. *Proc. Natl. Acad. Sci. U.S.A.* **94**, 10786–10791 (1997).
9. Y. Marahrens, B. Stillman, A yeast chromosomal origin of DNA replication defined by multiple functional elements. *Science* **255**, 817–823 (1992).
10. W. Xu, J. G. Aparicio, O. M. Aparicio, S. Tavaré, Genome-wide mapping of ORC and Mcm2p binding sites on tiling arrays and identification of essential ARS consensus sequences in *S. cerevisiae*. *BMC Genomics* **7**, 276 (2006).
11. J. J. Blow, R. A. Laskey, A role for the nuclear envelope in controlling DNA replication within the cell cycle. *Nature* **332**, 546–548 (1988).
12. I. Ilves, T. Petojevic, J. J. Pesavento, M. R. Botchan, Activation of the MCM2-7 helicase by association with Cdc45 and GINS proteins. *Mol. Cell* **37**, 247–258 (2010).
13. S. E. Moyer, P. W. Lewis, M. R. Botchan, Isolation of the Cdc45/Mcm2-7/GINS (CMG) complex, a candidate for the eukaryotic DNA replication fork helicase. *Proc. Natl. Acad. Sci. U.S.A.* **103**, 10236–10241 (2006).

14. L. D. Langston, M. E. O'Donnell, An explanation for origin unwinding in eukaryotes. *eLife* **8**, e46515 (2019).
15. J. S. Lewis *et al.*, Mechanism of replication origin melting nucleated by CMG helicase assembly. *Nature* **606**, 1007–1014 (2022).
16. N. M. Berbenetz, C. Nislow, G. W. Brown, Diversity of eukaryotic DNA replication origins revealed by genome-wide analysis of chromatin structure. *PLoS Genet.* **6**, e1001092 (2010).
17. A. M. Breier, S. Chatterji, N. R. Cozzarelli, Prediction of *Saccharomyces cerevisiae* replication origins. *Genome Biol.* **5**, R22 (2004).
18. J. A. Belsky, H. K. MacAlpine, Y. Lubelsky, A. J. Hartemink, D. M. MacAlpine, Genome-wide chromatin footprinting reveals changes in replication origin architecture induced by pre-RC assembly. *Genes Dev.* **29**, 212–224 (2015).
19. M. L. Eaton, K. Galani, S. Kang, S. P. Bell, D. M. MacAlpine, Conserved nucleosome positioning defines replication origins. *Genes Dev.* **24**, 748–753 (2010).
20. J. R. Lipford, S. P. Bell, Nucleosomes positioned by ORC facilitate the initiation of DNA replication. *Mol. Cell* **7**, 21–30 (2001).
21. C. F. Kurat, J. T. P. Yeeles, H. Patel, A. Early, J. F. X. Diffley, Chromatin controls DNA replication origin selection, lagging-strand synthesis, and replication fork rates. *Mol. Cell* **65**, 117–130 (2017).
22. S. Li *et al.*, Nucleosome-directed replication origin licensing independent of a consensus DNA sequence. *Nat. Commun.* **13**, 4947 (2022).
23. P. T. Lowary, J. Widom, New DNA sequence rules for high affinity binding to histone octamer and sequence-directed nucleosome positioning. *J. Mol. Biol.* **276**, 19–42 (1998).
24. I. F. Azmi *et al.*, Nucleosomes influence multiple steps during replication initiation. *eLife* **6**, e22512 (2017).
25. J. B. Crickard, C. J. Moevus, Y. Kwon, P. Sung, E. C. Greene, Rad54 drives ATP hydrolysis-dependent DNA sequence alignment during homologous recombination. *Cell* **181**, 1380–1394. e18 (2020).
26. P. N. Dyer *et al.*, Reconstitution of nucleosome core particles from recombinant histones and DNA. *Methods Enzymol.* **375**, 23–44 (2004).
27. S. Li, E. B. Zheng, L. Zhao, S. Liu, Nonreciprocal and conditional cooperativity directs the pioneer activity of pluripotency transcription factors. *Cell Rep.* **28**, 2689–2703.e4 (2019).
28. D. Duzdevich *et al.*, The dynamics of eukaryotic replication initiation: Origin specificity, licensing, and firing at the single-molecule level. *Mol. Cell* **58**, 483–494 (2015).
29. C. R. Clapier, J. Iwasa, B. R. Cairns, C. L. Peterson, Mechanisms of action and regulation of ATP-dependent chromatin-remodelling complexes. *Nat. Rev. Mol. Cell Biol.* **18**, 407–422 (2017).
30. J. Zlatanova, T. C. Bishop, J. M. Victor, V. Jackson, K. van Holde, The nucleosome family: Dynamic and growing. *Structure* **17**, 160–171 (2009).
31. C. Speck, Z. Chen, H. Li, B. Stillman, ATPase-dependent cooperative binding of ORC and Cdc6 to origin DNA. *Nat. Struct. Mol. Biol.* **12**, 965–971 (2005).
32. S. K. Bhardwaj *et al.*, Dinucleosome specificity and allosteric switch of the ISW1a ATP-dependent chromatin remodeler in transcription regulation. *Nat. Commun.* **11**, 5913 (2020).
33. I. Albert *et al.*, Translational and rotational settings of H2A.Z nucleosomes across the *Saccharomyces cerevisiae* genome. *Nature* **446**, 572–576 (2007).
34. H. Long *et al.*, H2A.Z facilitates licensing and activation of early replication origins. *Nature* **577**, 576–581 (2020).
35. P. De Ioannes *et al.*, Structure and function of the Orc1 BAH-nucleosome complex. *Nat. Commun.* **10**, 2894 (2019).
36. A. J. Kuo *et al.*, The BAH domain of ORC1 links H4K20me2 to DNA replication licensing and Meier-Gorlin syndrome. *Nature* **484**, 115–119 (2012).
37. P. Müller *et al.*, The conserved bromo-adjacent homology domain of yeast Orc1 functions in the selection of DNA replication origins within chromatin. *Genes Dev.* **24**, 1418–1433 (2010).
38. K. Hizume, M. Yagura, H. Araki, Concerted interaction between origin recognition complex (ORC), nucleosomes and replication origin DNA ensures stable ORC-origin binding. *Genes Cells* **18**, 764–779 (2013).
39. J. M. Cherry *et al.*, Saccharomyces Genome Database: The genomics resource of budding yeast. *Nucleic Acids Res.* **40**, D700–D705 (2012).
40. A. T. Spivak, G. D. Stormo, ScerTF: A comprehensive database of benchmarked position weight matrices for Saccharomyces species. *Nucleic Acids Res.* **40**, D162–D168 (2012).
41. R. V. Chereji, J. Ocampo, D. J. Clark, MNase-sensitive complexes in yeast: Nucleosomes and non-histone barriers. *Mol. Cell* **65**, 565–577.e3 (2017).
42. G. Mizuguchi *et al.*, ATP-driven exchange of histone H2AZ variant catalyzed by SWR1 chromatin remodeling complex. *Science* **303**, 343–348 (2004).
43. H. Li, B. Stillman, The origin recognition complex: A biochemical and structural view. *Subcell. Biochem.* **62**, 37–58 (2012).
44. R. T. Simpson, Nucleosome positioning can affect the function of a cis-acting DNA element in vivo. *Nature* **343**, 387–389 (1990).
45. J. F. Flanagan, C. L. Peterson, A role for the yeast SWI/SNF complex in DNA replication. *Nucleic Acids Res.* **27**, 2022–2028 (1999).
46. Y. Colino-Sanguino, S. J. Clark, F. Valdes-Mora, The H2A.Z-nucleosome code in mammals: Emerging functions. *Trends Genet.* **38**, 273–289 (2022).
47. Z. Zhang, M. K. Hayashi, O. Merkel, B. Stillman, R. M. Xu, Structure and function of the BAH-containing domain of Orc1p in epigenetic silencing. *EMBO J.* **21**, 4600–4611 (2002).
48. M. R. Wasserman, G. D. Schauer, M. E. O'Donnell, S. Liu, Replication fork activation is enabled by a single-stranded DNA gate in CMG helicase. *Cell* **178**, 600–611.e16 (2019).